

# ESTCP

# Cost and Performance Report

(ER-200702)



## Application of Advanced Sensor Technology to DoD Soil Vapor Intrusion Problems

October 2012



ENVIRONMENTAL SECURITY  
TECHNOLOGY CERTIFICATION PROGRAM

U.S. Department of Defense

## Report Documentation Page

*Form Approved  
OMB No. 0704-0188*

Public reporting burden for the collection of information is estimated to average 1 hour per response, including the time for reviewing instructions, searching existing data sources, gathering and maintaining the data needed, and completing and reviewing the collection of information. Send comments regarding this burden estimate or any other aspect of this collection of information, including suggestions for reducing this burden, to Washington Headquarters Services, Directorate for Information Operations and Reports, 1215 Jefferson Davis Highway, Suite 1204, Arlington VA 22202-4302. Respondents should be aware that notwithstanding any other provision of law, no person shall be subject to a penalty for failing to comply with a collection of information if it does not display a currently valid OMB control number.

1. REPORT DATE <b>OCT 2012</b>	2. REPORT TYPE <b>N/A</b>	3. DATES COVERED <b>-</b>						
4. TITLE AND SUBTITLE <b>Application of Advanced Sensor Technology to DoD Soil Vapor Intrusion Problems</b>								
6. AUTHOR(S)								
7. PERFORMING ORGANIZATION NAME(S) AND ADDRESS(ES) <b>ESTCP Office 4800 Mark Center Drive Suite 17D08 Alexandria, VA 22350-3605</b>								
9. SPONSORING/MONITORING AGENCY NAME(S) AND ADDRESS(ES)								
12. DISTRIBUTION/AVAILABILITY STATEMENT <b>Approved for public release, distribution unlimited</b>								
13. SUPPLEMENTARY NOTES <b>The original document contains color images.</b>								
14. ABSTRACT								
15. SUBJECT TERMS								
16. SECURITY CLASSIFICATION OF: <table border="1" style="width: 100%; border-collapse: collapse;"> <tr> <td style="width: 33%;">a. REPORT <b>unclassified</b></td> <td style="width: 33%;">b. ABSTRACT <b>unclassified</b></td> <td style="width: 34%;">c. THIS PAGE <b>unclassified</b></td> </tr> </table>			a. REPORT <b>unclassified</b>	b. ABSTRACT <b>unclassified</b>	c. THIS PAGE <b>unclassified</b>	17. LIMITATION OF ABSTRACT <b>SAR</b>	18. NUMBER OF PAGES <b>45</b>	19a. NAME OF RESPONSIBLE PERSON
a. REPORT <b>unclassified</b>	b. ABSTRACT <b>unclassified</b>	c. THIS PAGE <b>unclassified</b>						

# **COST & PERFORMANCE REPORT**

Project: ER-200702

## **TABLE OF CONTENTS**

	<b>Page</b>
1.0 EXECUTIVE SUMMARY .....	1
2.0 INTRODUCTION .....	3
2.1 BACKGROUND .....	3
2.2 OBJECTIVE OF THE DEMONSTRATION .....	4
2.3 REGULATORY DRIVERS .....	4
3.0 TECHNOLOGY .....	7
3.1 TECHNOLOGY DESCRIPTION .....	7
3.2 ADVANTAGES AND LIMITATIONS OF THE TECHNOLOGY .....	9
4.0 PERFORMANCE OBJECTIVES .....	12
5.0 SITE DESCRIPTION .....	14
6.0 TEST DESIGN .....	16
6.1 CONCEPTUAL EXPERIMENTAL DESIGN .....	16
6.2 LABORATORY STUDY RESULTS .....	16
6.3 FIELD TESTING .....	19
6.4 FIELD SAMPLING METHODS .....	20
6.5 FIELD SAMPLING RESULTS .....	21
7.0 PERFORMANCE ASSESSMENT .....	26
8.0 COST ASSESSMENT .....	29
8.1 COST MODEL .....	29
8.2 COST DRIVERS .....	30
8.3 COST ANALYSIS .....	30
9.0 IMPLEMENTATION ISSUES .....	31
10.0 REFERENCES .....	33
APPENDIX A                   POINTS OF CONTACT .....	A-1

## LIST OF FIGURES

	<b>Page</b>
Figure 1. Fluidic diagram of $\mu$ GC key components showing the front-end sampling and analytical subsystems.....	7
Figure 2. Photographs of major components.....	8
Figure 3. Schematics illustrating a) MPN chemiresistor processes; b) response patterns generated from different chemiresistors.....	8
Figure 4. (a) SPIRON prototype $\mu$ GC and laptop; and (b) chromatograms generated by $\mu$ GC.....	9
Figure 4. Map of Hill AFB, Utah, with surrounding communities.....	14
Figure 5. Prototype SPIRON $\mu$ GC system and components.....	17
Figure 6. Operational mode fluidic flow paths for the SPIRON $\mu$ GC.....	17
Figure 7. SEM images of the etched-Si channels used in the 3-meter-long $\mu$ columns prior to sealing and coating with stationary phase.....	18
Figure 8. Photographs of the CR array.....	19
Figure 9. a) TCE Calibration curves for $\mu$ GC prototype (inset shows TCE peaks for 20 Liter [L] 0.12 ppb TCE); and b) chromatograms from the four CR sensors for analysis of TCE and other VOCs.....	19
Figure 10. Photographs of: a) Layton, Utah, ASU SERDP project study house and b) basement storage closet beneath stairs with significant VI entry location.....	20
Figure 11. Field TCE calibration curves.....	21
Figure 12. Results of periodic analysis of the TCE tank standard (2-L sample; 9.6 ppb TCE) showing a) stability of responses and b) relative response patterns over the 3-week field study.....	22
Figure 13. a) Representative chromatograms from the MPN-coated CR array for a field measurement having 12 ppb TCE; and b) response patterns for TCE and unknown VOCs with pattern-matching correlation coefficients ( $r$ ). Bars left to right: C8, DPA, OPH, and HME.....	22
Figure 14. Correlation of pooled TCE measurements from $\mu$ GC prototypes and corresponding TO-15 samples.....	23
Figure 15. Correlations of the pooled TCE measurements from $\mu$ GC prototypes with corresponding TO-15 results for data pair subsets a) TCE >MAL and $r >0.85$ , b) TCE <MAL and $r >0.85$ , and c) TCE <MAL and $r <0.85$ (MAL 2.3 ppb at time of field demonstration).....	23
Figure 16. Extracted subsections of several chromatograms from the OPH sensor of Proto 1 and corresponding normalized response patterns from the CR array (insets) for TCE peaks .....	24
Figure 17. Results of 48 hours of continuous, automated (unattended) TCE concentration measurements with Proto 1 (open triangles, crawl space) and Proto 2 (filled triangles, hallway), along with measurements by TO-15 (open circles, crawl space) and portable GC/MS (filled circles, hallway) as a function of differential pressure (indoor relative to sub-slab; line).....	24
Figure 18. Spatial distributions of TCE in Layton, Utah, house without VI and emplaced indoor source of TCE. ....	25

## LIST OF FIGURES (continued)

	<b>Page</b>
Figure 19. Correlation between TO-15 and $\mu$ GC prototype TCE field sample results for a) TO-15 results greater than 10 times $\mu$ GC LOD, and b) TO-15 results less than 10 times $\mu$ GC LOD.....	27

## LIST OF TABLES

	<b>Page</b>
Table 1.	Quantitative performance objectives. ....
Table 2.	Qualitative performance objectives. ....
Table 3.	LOD for TCE with both $\mu$ GC prototypes in the field for assumed sample volumes of 4 L and 20 L (in parentheses).....
Table 4.	Cost model for short-term forensic-type application of $\mu$ GC for VI.....
Table 5.	Cost model for long-term monitoring application of $\mu$ GC for VI.....

## ACRONYMS AND ABBREVIATIONS

---

°C	degrees Celsius
μcolumns	microfabricated columns
μarray	micro-array
μdetector	micro-detector
μF	micro-focuser
μGC	micro-gas chromatograph
μg/m <sup>3</sup>	micrograms per cubic meter
AFB	Air Force Base
ASU	Arizona State University
ATSDR	Agency for Toxic Substances and Disease Registry
Au	gold
CDPHE	Colorado Department of Public Health and Environment
Cr	chromium
CR	chemiresistor
C8	n-octane
DoD	U.S. Department of Defense
DPA	4-mercaptodiphenylacetylene
ESTCP	Environmental Security Technology Certification Program
ETV	Environmental Technology Verification
GC	gas chromatography
GC/MS	gas chromatography/mass spectrometry
HFA	
HME	methyl-6-mercaptopentanoate
IST	Integrated Science and Technology
L	liter
L/min	liter per minute
LOD	limit of detection
M	meta
MAL	mitigation action level
MCR	multivariate curve resolution
mg	milligram
MPN	thiolate-monolayer-protected gold nanoparticles
MS	mass spectrometry
nm	nanometer

## ACRONYMS AND ABBREVIATIONS (continued)

---

OPH	1-mercaptop-6-phenoxyhexane
PCE	tetrachloroethylene
PCF	preconcentrator/focuser
ppb	parts per billion
ppt	parts per trillion
Pt	platinum
QA	quality assurance
QC	quality control
r	correlation coefficient
RSD	relative standard deviation
RV	recreational vehicle
SEM	scanning electron microscope
SERDP	Strategic Environmental Research and Development Program
TCE	trichloroethylene
Ti	titanium
TO-15	Toxic Organics-15
TO-17	Toxic Organics-17
USEPA	U.S. Environmental Protection Agency
VI	vapor intrusion
VOC	volatile organic compound

## ACKNOWLEDGEMENTS

The inspiration behind this project was provided by Dr. Rob Hinchee (Integrated Science and Technology [IST]) and Kyle Gorder (Hill Air Force Base [AFB]). Kyle's logistical/technical assistance and encouragement was crucial to this project and is gratefully acknowledged. Dr. Erik Dettenmaier's (Hill AFB) technical assistance with HAPSITE gas chromatography/mass spectrometry (GC/MS) field data collection is much appreciated.

Dr. Paul Johnson's (Arizona State University [ASU]) technical advice and use of ASU's Strategic Environmental Research and Development Program (SERDP) VI study house in Layton, Utah, is very gratefully acknowledged, as well as the technical assistance of Dr. Paul Dahlen (ASU).

The University of Michigan "team" was instrumental in the development, fabrication, and lab and field testing of the SPIRON micro-gas chromatograph ( $\mu$ GC) prototypes and contributions of the various team members are gratefully acknowledged. Dr. Hungwei Chang was crucial in the fabrication of the  $\mu$ GC prototypes. Doctoral candidate Sun Kyu Kim's efforts in the laboratory and field testing of the  $\mu$ GC prototypes were central to the success of this project. Thitiporn Sukaew led efforts towards the design and testing of front-end multi-stage preconcentrator/focuser. Jonathan Bryant provided technical assistance for several aspects the project especially the start-up of the field demonstration. Jun Hwan Seo and Katsuo helped design and model the micro-focuser ( $\mu$ F). Katharine Beach fabricated the  $\mu$ Fs. Gustavo Serrano, Forest Bohrer, Brendan Casey, Robert Gordenker and Brad Richert contributed their technical expertise to various aspect of the project. The field efforts of David Wolf (IST) are also gratefully acknowledged.

Additional support towards this project was provided by Engineering Research Centers Program of the National Science Foundation under Award Number ERC-9986866 (University of Michigan's Center for Wireless Integrated MicroSystems). The micro-fabricated devices described in this report were made in University of Michigan's Lurie Nanofabrication Facility, a member of the National Nanotechnology Infrastructure Network, which is supported by the National Science Foundation.

*Technical material contained in this report has been approved for public release.  
Mention of trade names or commercial products in this report is for informational purposes only;  
no endorsement or recommendation is implied.*

*This page left blank intentionally.*

## 1.0 EXECUTIVE SUMMARY

Vapor intrusion (VI) of groundwater contaminants like trichloroethylene (TCE) has become an issue of increasing concern over the past decade necessitating development of methods to appropriately evaluate it. Determination of TCE concentrations in indoor air can be a crucial part of VI assessments. The conventional and most commonly used U.S. Environmental Protection Agency (USEPA) Toxic Organics-15 (TO-15) (gas chromatography/mass spectrometry [GC/MS]) method is limited primarily by protracted turnaround times, multiple house visits, and per-sample cost. Near-real-time on-site analysis can address these concerns and identify potential interfering indoor sources as well. A commercially available portable GC/MS provides a near-real time analysis, but has high capital costs, requires external carrier gas, and can have significant instrument downtime for costly maintenance. The overall project objective was to evaluate the efficacy of a micro-gas chromatograph ( $\mu$ GC) prototype for detection of low-level TCE concentrations in indoor-air VI applications as a potential cost-effective alternative.

The  $\mu$ GC prototype, developed by the University of Michigan, consists of a conventional sampling front-end module and a novel micro-analysis module. The front-end sampling module concentrates volatile organic compounds (VOC) in the TCE vapor pressure range. A microfabricated micro-focuser ( $\mu$ F) injects the sample onto the separation microfabricated columns ( $\mu$ columns) with independent temperature control; scrubbed air is used as the carrier gas. The micro-detector ( $\mu$ detector) consists of an array of four different chemiresistor (CR) sensors, thus providing compound-specific response patterns. Both modules are controlled by customized software. Laboratory  $\mu$ GC studies showed that TCE detection limits in the low- and sub-parts per billion (ppb) range could be obtained and that the  $\mu$ GC was applicable to analysis of other VOCs.

A field demonstration was conducted in the vicinity of Hill Air Force Base (AFB), Utah; primarily in a house with known TCE VI. Concurrent reference samples were analyzed by TO-15. Field calibration detection limits were similar to those in the laboratory. TCE levels were varied by creating a negative indoor air pressure relative to sub-slab. Comparison with concurrent TO-15 samples showed that the  $\mu$ GC prototype TCE accuracy was good above its TCE mitigation action level (MAL) (2.3 ppb; at time of field demonstration), but less accurate below 1 ppb due to interfering VOCs. Long-term results showed that response stability was adequate and could be improved with  $\mu$ detector temperature control. Temporal and spatial studies were conducted. Temporal TCE variations were effectively tracked by the  $\mu$ GC; including a 48-hour unattended, automated run. Spatial studies showed concentration gradients indicating VI entry and an emplaced indoor TCE source. These studies illustrate the efficacy of the  $\mu$ GC prototype in real-world VI applications.

A primary implementation issue is that the  $\mu$ GC is not currently commercially available. Future work is needed to further reduce its size, improve ease of use, improve robustness, incorporate remote communications, and implement hardware and software refinements to improve accuracy. Using cost estimates, a commercial  $\mu$ GC for VI applications is anticipated to be more cost-effective than the traditional TO-15 approach.

This study stands as the first of its kind, where  $\mu$ GC instrumentation was shown capable of sustained, reliable, automated measurements of a trace-level component (TCE) in a complex VOC mixture under field conditions.  $\mu$ GC technology holds great promise for environmental monitoring problems (e.g., VI) where speciated low-concentration measurements are required.

## 2.0 INTRODUCTION

### 2.1 BACKGROUND

Indoor air VI is the entry of VOCs into buildings overlying contaminated soils or groundwater. VI has been an emerging problem, the extent of which has been more fully recognized by U.S. Department of Defense (DoD), regulators, private industry, and others over the past decade. A number of DoD facilities have VI issues, and TCE is a common VI contaminant. Target regulatory action levels for some compounds of concern, such as TCE, are in the low ppb to parts per trillion (ppt) range. Current sampling and analysis methods, including TO-15 and Toxic Organics-17 (TO-17), are sufficiently sensitive and selective in a complex matrix such as indoor air, however they have limitations in VI applications including: cost, shipment to an off-site laboratory, and delayed results. These limitations can adversely impact forensic determination of indoor sources and exposure estimation where concentrations vary due to changing conditions.

Indoor air concentrations of the intruding VOCs are typically low but may pose unacceptable risks. Evaluation of potential risk due to VI is complicated since vapors may be due to non-VI sources. TCE can be found in a number of common household products (Agency for Toxic Substances and Disease Registry [ATSDR], 1997; Colorado Department of Public Health and Environment [CDPHE], 2005); thus, it is challenging to differentiate TCE due to VI from background sources. Presence in indoor air does not confirm a completed VI pathway. In 2002, the USEPA issued draft VI Guidance (USEPA, 2002). Insights gained from numerous field investigations, including those on temporal and spatial variability, were used in a USEPA review of its guidance (USEPA, 2010), which encourages addressing background sources and earlier indoor air sampling efforts in site screening. Evaluating the VI pathway involves sampling immediately outside and inside buildings, which can be invasive and inconvenient to the building occupants. Minimizing the invasive nature of VI investigations can improve community relations and risk communications.

Indoor air quality criteria vary between regulatory jurisdictions and over time. At Hill AFB (this project's demonstration site), the MAL (concentration above which action is to be taken to mitigate VI) at the time of the field demonstration for TCE was 12.6 micrograms per cubic meter ( $\mu\text{g}/\text{m}^3$ ) (2.3 ppb) (Note: TCE risk values have changed since the field demonstration, so for continuity the report is written from the standpoint of the MAL in place at the time of the demonstration; and for clarity the newer, lower MAL value of  $2.1 \mu\text{g}/\text{m}^3$  or 0.38 ppb, will also be noted.). Implementation of commonly applied VI mitigation measures cannot decrease indoor air contaminant concentrations from indoor sources; lack of effectiveness of an installed mitigation system is suggestive of an indoor vapor source. A portable field instrument that can rapidly measure low TCE concentrations can aid in identifying and locating indoor TCE sources.

The only currently available commercial field instrument sufficiently sensitive and selective for use in VI applications is the HAPSITE field portable GC/MS. Hill AFB has been using the HAPSITE over the past several years in their VI investigations and has found it useful, particularly in locating indoor sources (Kyle Gorder, Hill AFB, personal communication; Environmental Security Technology Certification Program [ESTCP] Project ER-201119; Gorder

and Dettenmaier, 2011). Limitations of the HAPSITE include high capital costs, pressurized carrier gas, intensive operator training, and frequent repairs.

This technology demonstration project examines the applicability of an innovative miniaturized instrument for on-site measurements of trace levels of TCE in dwellings. The instrument, developed at the University of Michigan and dubbed SPIRON, is a gas chromatograph whose principal components are microfabricated – a  $\mu$ GC. SPIRON  $\mu$ GC prototypes were demonstrated in two modes: 1) portable mode for near-real-time determinations of TCE to identify sources (spatial variations); and 2) fixed-location mode for continuous TCE monitoring (temporal variations). Field demonstration was conducted primarily in a house in the vicinity of Hill AFB with TCE VI. Concurrent reference method TO-15 sampling/analysis allowed for a thorough evaluation of  $\mu$ GC performance under real-world conditions.

## **2.2 OBJECTIVE OF THE DEMONSTRATION**

SPIRON  $\mu$ GC prototypes optimized for TCE were fabricated specifically for this demonstration to be used in the portable  $\mu$ GC mode for near-real time contaminant source assessment (forensic) and spatial concentration distributions and the fixed-location  $\mu$ GC mode for long-term temporal concentration monitoring (exposure estimation).

The objective of the demonstration was to field-validate the SPIRON  $\mu$ GC in its portable and fixed-location operational modes in addressing TCE VI problems. The field demonstration for performance evaluation of the fixed-location  $\mu$ GC mode (temporal concentrations) was conducted in a TCE VI-impacted house near Hill AFB. The field demonstration for performance evaluation of the portable  $\mu$ GC mode (spatial concentrations) was conducted in the VI-impacted study house as well as a second nearby house in which a TCE indoor source was emplaced.

A more over-arching objective of this demonstration was to facilitate the continued development and improvements in  $\mu$ GC technology for environmental applications, including VI. The SPIRON  $\mu$ GC is a prototype developed by University of Michigan and is not a commercially available instrument. The  $\mu$ GC prototype demonstration can facilitate technology transfer by encouraging analytical instrumentation manufacturers who are currently or considering pursuing  $\mu$ GC technologies to produce cost-effective  $\mu$ GCs for VI and other environmental applications. DoD facilities and the private sector would benefit by having access to powerful, low-cost field VOC analytical tools for VI specifically, and other environmental applications in general.

## **2.3 REGULATORY DRIVERS**

Federal and state regulatory agency response to VI has evolved to require better assessment and mitigation of potential risks. USEPA has issued Draft Subsurface Vapor Intrusion Guidance (USEPA, 2002); a recent review (USEPA, 2010) indicates revision will include increased emphasis on indoor air analysis to be done earlier in the screening process along with temporal and spatial variability assessment.

MALs vary by jurisdiction. The Hill AFB vicinity MAL at the time of the field demonstration was 2.3 ppb (currently it has been lowered to 0.38 ppb based upon a recent USEPA evaluation of TCE risk).

*This page left blank intentionally.*

## 3.0 TECHNOLOGY

Recent advances in  $\mu$ GC technology made it a suitable choice for the quantification of TCE in indoor air for this project's portable and long-term fixed-location VI applications.  $\mu$ GC approaches do not require supplied carrier gas. Rather, they can use scrubbed ambient air as the carrier.  $\mu$ GC technologies also have the advantage of smaller size and lower power requirements. Further evolution of  $\mu$ GC technology can contribute to environmental applications beyond those of VI.

### 3.1 TECHNOLOGY DESCRIPTION

Front-end sampler and analytical subsystems comprise the basic components of the prototype  $\mu$ GC. A fluidic diagram is shown in Figure 1. The front-end sampler subsystem and the  $\mu$ F are referred as the multi-stage preconcentrator/focuser (PCF) module. Key components and the PC-board mounted micro-analytical subsystem are shown in Figure 2.

Laboratory development and characterization of the multi-stage PCF module and the SPIRON prototype  $\mu$ GC are presented in Sukaew et al., 2011 and Kim et al., 2011, respectively. The multi-stage PCF performs three vital functions: 1) prevents low vapor pressure compounds from entering analysis module; 2) traps TCE (and similar vapor pressure compounds); and 3) injects the sample into the analytical module. The pre-trap (Carbopack B) prevents VOCs with lower vapor pressures from entering the analytical module. The high-volume sampler (Carbopack X) traps TCE (and similar compounds) while allowing compounds with higher vapor pressures to flow through and not be trapped. After sample collection the flow is reversed with scrubbed ambient air flowing through the sampler to the  $\mu$ F (Carbopack X) and the sampler is heated to transfer the sample onto the  $\mu$ F. The  $\mu$ F is rapidly heated to inject the sample on the analytical subsystem. The pre-trap and sampler are of conventional design and the  $\mu$ F is microfabricated.

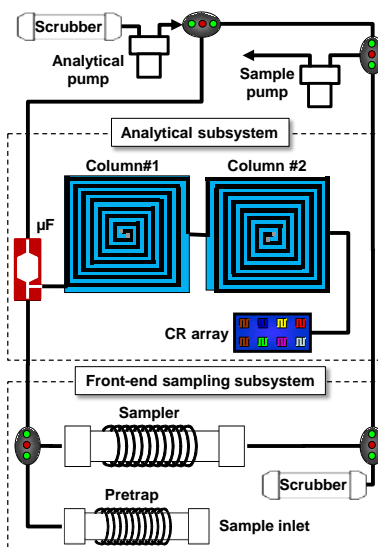


**Figure 1.** Fluidic diagram of  $\mu$ GC key components showing the front-end sampling and analytical subsystems.

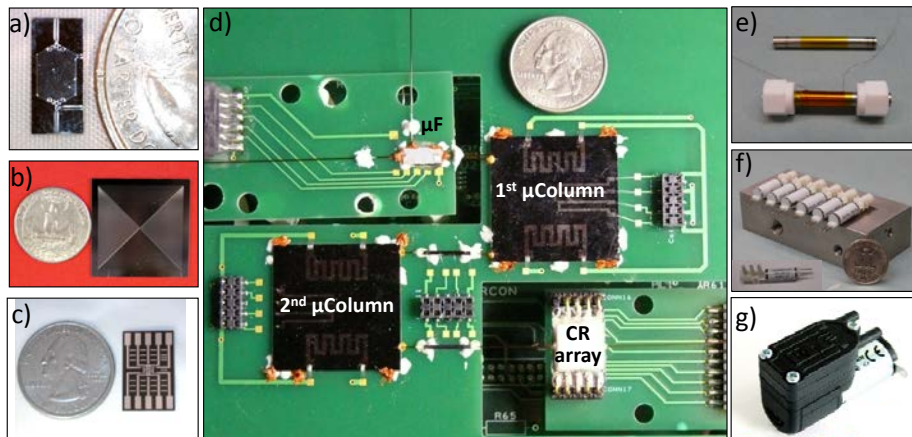


**Figure 2. Photographs of major components.**

- a)  $\mu$ F; b) 3 m microcolumn; c) microsensor array detector;
- d) integrated micro-analytical subsystem; e) high-volume sampler/pretrap;
- f) valve and valve manifold; g) miniature diaphragm pump.

The SPIRON prototype  $\mu$ GC has two, 3-m  $\mu$ columns with integrated thin-film heaters. The  $\mu$ F-injected compounds are separated in the  $\mu$ columns due to partitioning between the stationary phase and the mobile carrier gas (scrubbed ambient air). The  $\mu$ columns are temperature programmed to facilitate the migration of compounds through the columns. As the compounds exit the columns, they pass across the microsensor array for detection. The microsensor array has four CRs each employing different thiolate-monolayer-protected gold nanoparticles (MPN) as sorptive interface layers coating indigital electrodes. Each CR responds with partial selectivity to different compounds. As each eluting vapor enters the detector cell that houses the sensor array, it rapidly and reversibly partitions into the MPN films, causing them to swell changing the film resistance which is measured. Figure 3a illustrates various processes of MPN CRs as they function as a gas chromatography (GC) detector. Figure 3b illustrates a set of hypothetical responses (forming a collective pattern) generated from an array of MPN-coated CRs. The four thiol functionalities used in this study are: n-octane (C8), 4-mercaptop diphenylacetylene (DPA), 1-mercaptop-6-phenoxyhexane (OPH), and methyl-6-mercaptophexanoate (HME).

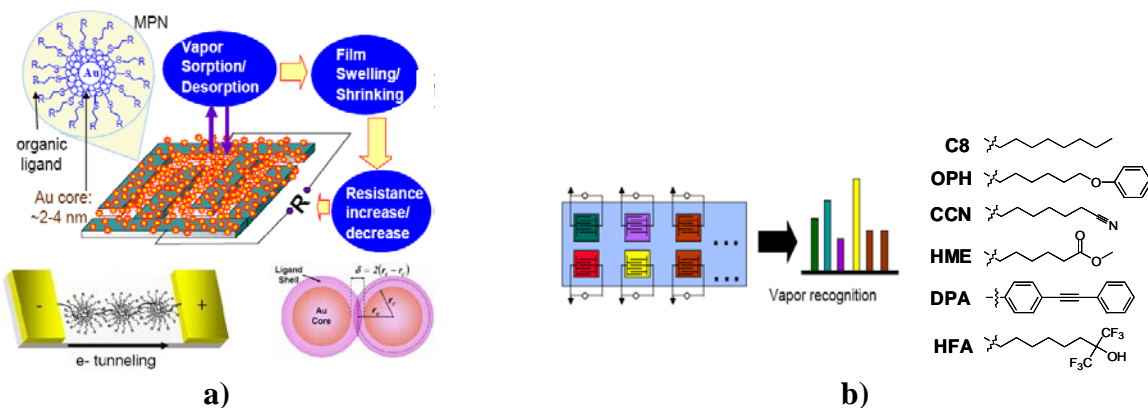


**Figure 3. Schematics illustrating a) MPN CR processes; b) response patterns generated from different CRs.**

Quantification can be based on either peak height or peak area. One of the SPIRON prototype  $\mu$ GCs is shown in Figure 4a. Figure 4b shows the chromatographic traces generated by the SPIRON prototype  $\mu$ GC for an air sample containing 2-butanone, benzene, TCE, tetrachloroethylene (PCE), ethylbenzene and meta (m)-xylene, as well as several of their response patterns.

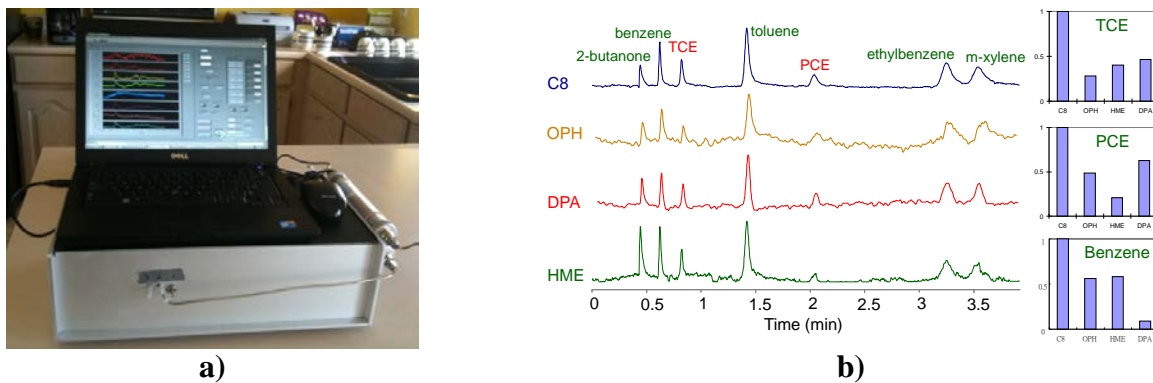


**Figure 4. a) SPIRON prototype  $\mu$ GC and laptop; and b) chromatograms generated by  $\mu$ GC.**

Histograms illustrate relative response patterns for TCE, PCE, and benzene.

### 3.2 ADVANTAGES AND LIMITATIONS OF THE TECHNOLOGY

Currently, cost-effective, sensitive, and compound-selective tools for efficient field investigation and assessment of VI problems do not exist. Mobile analytical laboratories (van, recreational vehicle [RV], trailer) are available, but can be obtrusive and costly. The HAPSITE GC/MS has proven useful in VI applications but is costly, can have significant downtime, and requires substantial training. The  $\mu$ GC provides substantial advantages over the commonly used traditional TO-15 analysis approach which has limitations (few data points, multiple site visits, limited as a forensic tool, limited exposure assessment capability, cost, and time delay in obtaining results); however, TO-15 will still be needed in many VI applications. The  $\mu$ GC may outperform current portable GCs on the market in terms of ease-of-use, lower level of operator training required, sensitivity, selectivity, cost, and sample turnaround. The  $\mu$ GC is anticipated to lead to a paradigm shift in environmental, health and safety, and on-site VOC analysis at industrial operations.

In terms of limitations, the  $\mu$ GC is currently in the prototype stage and is not commercially available. Results of this technology demonstration should facilitate regulatory and practitioner acceptance of  $\mu$ GC data for VI and other environmental applications; and encourage potential manufacturers to produce commercial field-worthy  $\mu$ GCs. Improvements are needed in specific compound quantification accuracy in the presence of potential interferents in the low concentration range (e.g., improved resolution, sensor selectivity/sensitivity, chemometrics), particularly in light of the lowering of the Hill AFB TCE MAL since the field demonstration from 2.3 ppb to 0.38 ppb. Practical application of new and evolving  $\mu$ GC technologies to VI

(and other environmental applications) can only be realized through commercial production of  $\mu$ GCs that meets the needs of these applications.

*This page left blank intentionally.*

## 4.0 PERFORMANCE OBJECTIVES

Quantitative and qualitative performance objectives for this technology demonstration are given below in Tables 1 and 2, respectively.

**Table 1. Quantitative performance objectives.**

Performance Objective	Data Requirements	Success Criteria
Sensitivity to TCE – portable µGC mode	Laboratory determination of LOD <sup>a</sup> for TCE	≤0.06 ppb TCE LOD
Sensitivity to TCE – fixed-location µGC Mode	Laboratory determination of LOD for TCE	≤0.03 ppb TCE LOD
Evaluating µGC response stability	Periodic collection of µGC and TO-15 data on TCE standardization gas	Relative standard deviation of µGC responses of 20% or less
Correlation of TCE field sample results for µGC and TO-15 results	Periodic collection of µGC and TO-15 data on the same in-house field indoor air samples	Agreement within factor of 1.43 for >10 times LOD (70-143%); Agreement within factor of 2 for <10 times LOD (50-200%); 20% failure rate acceptable

<sup>a</sup>limit of detection

**Table 2. Qualitative performance objectives.**

Performance Objective	Data Requirements	Success Criteria
Ease of use	Field team feedback	Single field technician sufficient
Ease of field standardization & blanks	Field team feedback	Effective and time-efficient
Rapid site assessment – portable µGC mode	Collection of field µGC and TO-15 TCE data in a forensic mode	Effective site assessment in house within 1 day
Long-term operation	Operational history under field conditions	Continuous operation of approximately 1 month

*This page left blank intentionally.*

## 5.0 SITE DESCRIPTION

Hill AFB, located in northern Utah, has been an active facility since the early 1940s. The base lies on a plateau roughly 300 ft above a valley floor and is surrounded by various residential communities. Figure 4 is a map of Hill AFB, groundwater plumes, and Arizona State University's (ASU) ESTCP and TCE Emplaced Source study house locations.

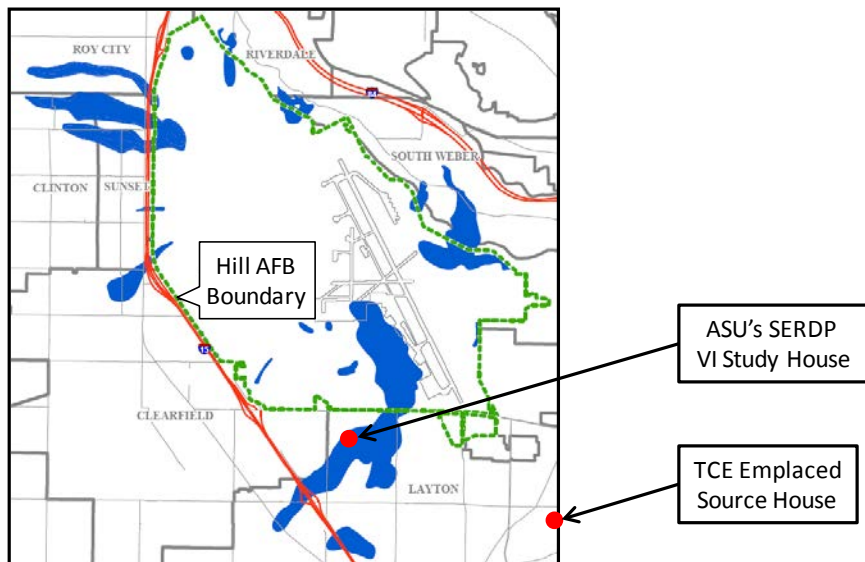


**Figure 4. Map of Hill AFB, Utah, with surrounding communities.**

Outline of base is represented by the green dashed line.

The blue areas are groundwater plumes, most with TCE contamination.

Locations of the residential houses used in this demonstration are indicated.

Aircraft maintenance activities at the base historically involved the use of TCE (and other solvents) to clean aircraft parts. Some the TCE used was disposed of into the ground at various locations around the base, creating groundwater plumes. As the base is on a plateau, groundwater tends to flow off-base to the lower lying valley floor, leading to shallow groundwater contamination in the surrounding residential areas. Shallow TCE groundwater contamination may lead to TCE migration from the groundwater to the overlying unsaturated (vadose) zone and potentially to soil vapor beneath houses. Neutral to negative pressures within houses relative to the soil gas pressures can lead to migration of TCE into houses, resulting in indoor air VI.

The majority of the field demonstration was conducted in the ASU Strategic Environmental Research and Development Program (ESTCP) VI study house (Dr. Paul Johnson, ASU, principal investigator), which is located in Layton, Utah, over a shallow TCE groundwater plume that has migrated to the south of Hill AFB (Figure 4). The presence of TCE in shallow groundwater and active TCE VI into this house (historical observed indoor air TCE concentrations ranged up to the low single digit ppb range) was confirmed by ASU and Hill AFB personnel during selection of the house for the SERDP project. A second house in Layton, UT without TCE VI (Figure 4) was also used in this demonstration. An indoor TCE source was intentionally emplaced (TCE

source location initially unknown to field team) in the second house to evaluate the µGC's ability to identify indoor TCE sources.

## 6.0 TEST DESIGN

### 6.1 CONCEPTUAL EXPERIMENTAL DESIGN

The primary goal of this project was to conduct a field performance evaluation of the SPIRON  $\mu$ GC prototype. In conjunction with the field component, laboratory testing of the SPIRON  $\mu$ GC was also conducted to evaluate its performance under controlled laboratory conditions. Additional laboratory work was also conducted after the field demonstration to better explore the potential for the use of multivariate curve resolution (MCR) to resolve overlapping (co-eluting) peaks and improve TCE quantification under typical field conditions.

This field demonstration was to evaluate the performance of the SPIRON  $\mu$ GC prototype in short-term portable forensic-type and longer-term fixed-location monitoring type applications to analyze indoor air TCE concentrations that may be the result of VI (or due to existing indoor TCE sources). The SPIRON  $\mu$ GC prototype (two prototypes were used in the field) was able to sample and analyze samples for TCE at a frequency substantially greater than is practicable using the TO-15 conventional approach. Periodic simultaneous sampling using  $\mu$ GC and TO-15 methodologies enabled comparison of TCE concentrations obtained by the two approaches. Potential TCE concentrations due to VI or indoor sources can vary greatly. The value of this field demonstration for  $\mu$ GC prototype performance evaluation was significantly enhanced by a relatively wide range of field TCE concentrations monitored by both the field  $\mu$ GC and TO-15 methods, as well as periodically with the portable HAPSITE GC/MS.

The  $\mu$ GC prototypes were calibrated for TCE in the field and the extent of response drift was assessed by periodic measurement of a TCE gas standard (also allowing for adjustments in TCE calibration factors). Periodic blanks were also analyzed. The portable  $\mu$ GC application (i.e., spatial concentration data) was conducted over several days at the ASU SERDP VI-study house and at a Layton, Utah, non-VI house with an emplaced indoor TCE source. The demonstration of the fixed-location  $\mu$ GC application entailed continuous TCE concentration monitoring to assess temporal in indoor air concentrations. The fixed  $\mu$ GCS were installed in near a main VI entry location in the ASU study house basement. For a 48-hour period, the  $\mu$ GC prototypes were operated in an automated mode to demonstrate continuous automated sampling and analysis.

### 6.2 LABORATORY STUDY RESULTS

The following describes key results generated during development and characterization of the SPIRON prototype  $\mu$ GC in a laboratory setting as described in Sukaew et al. (2011) and Kim et al. (2011) as well as post-field demonstration examination of MCR with the prototype  $\mu$ GC as described in Kim and Zellers. Components of the  $\mu$ GC prototype are shown in Figure 5 illustrating the sampling and analysis subsystems. The detector sensitivity requires preconcentration to achieve the detection limits required for VI applications; which is the case for all current  $\mu$ GC detector designs. Figure 6 shows the fluidic flow paths of the main modes of operation: sampling, focusing, and stabilization/analysis.

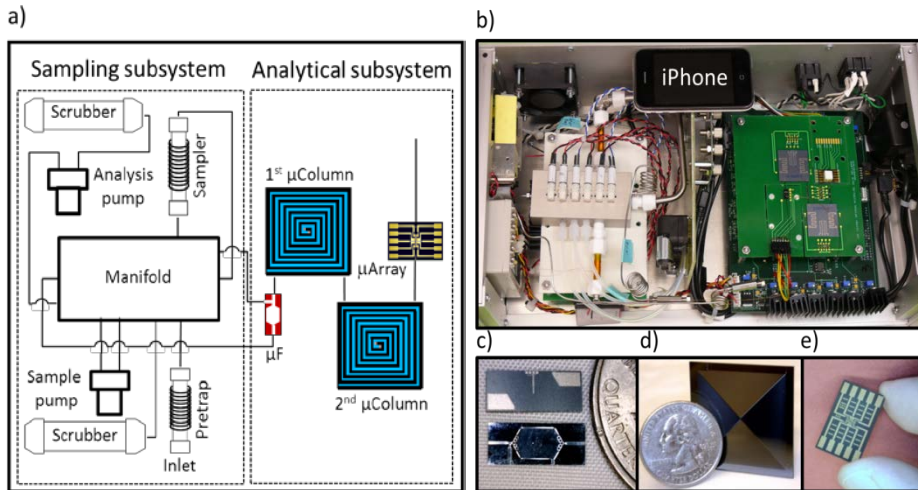


**Figure 5. Prototype SPIRON  $\mu$ GC system and components.**  
a) layout diagram showing subsystems and fluidic pathways;  
b) top view of Prototype 1 with cover panel removed (iPhone included for scale);  
c)  $\mu$ focuser; d)  $\mu$ column; and e) micro-scale CR array.

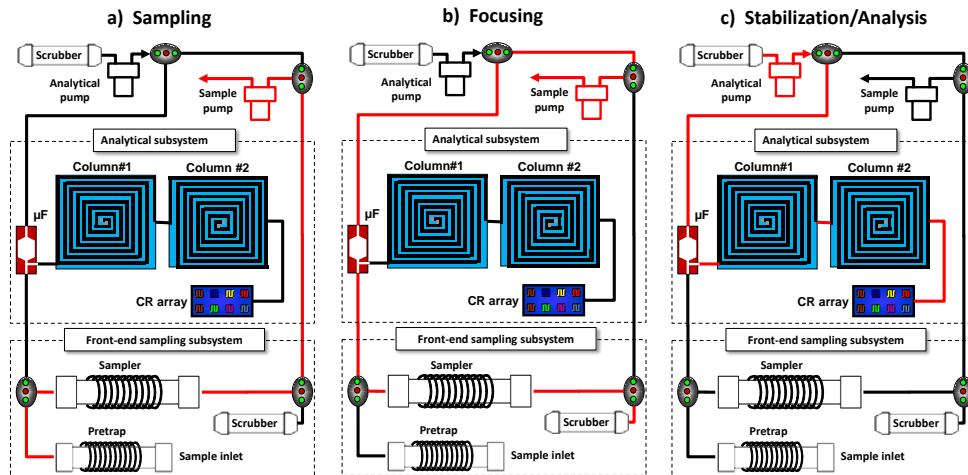


**Figure 6. Operational mode fluidic flow paths for the SPIRON  $\mu$ GC.**  
a) sampling, b) focusing, and c) stabilization/analysis

Development of the front-end sampling subsystem and its optimization for the preconcentration of TCE is detailed in Sukaew et al. (2011). The functions of the sampling subsystem are to: 1) prevent low vapor pressure VOCs from entering the analytical subsystem, 2) prevent VOCs with vapor pressures significantly higher than TCE from entering the analytical subsystem; and 3) to concentrate VOCs in the vapor pressures range including TCE from a large air sample (for greater preconcentration factor) and load those compounds onto the  $\mu$ F of the analytical subsystem.

The main components of the sampling subsystem are the pretrap and high-volume sampler, thin-walled stainless steel tubes (heated with coils of insulated copper wire and monitored with

thermocouples held snugly against the tube walls) with graphitized carbon adsorbents. In operation, a commercial mini-pump (miniature diaphragm pump, NMS020, KNF Neuburger, Trenton, New Jersey) draws an air sample through the pre-trap and sampler at a high flow rate (approximately 1 liter per minute [L/min]). The pretrap has a 50 mg bed of Carbopack B. Low vapor pressure compounds are captured by the pretrap (and periodically desorbed by heating with a reverse flow of scrubbed ambient air). The high-volume sampler has a 100 mg bed of Carbopack X. High vapor pressure VOCs are not retained on the sampler and exit the system while compounds with vapor pressures similar to TCE (3 to 100 torr range; TCE is 69 torr) are trapped on the sampler. After sampling a specified volume of air sample, the flow is re-configured from the sampler to the  $\mu$ F. Lower flow rate and sampler heating transfers TCE (and similar compounds) to the  $\mu$ F. The  $\mu$ F chip (Figure 5c) has a 3.2 (width)  $\times$  3.45 (length)  $\times$  0.38 mm (height) cavity with tapered sections leading to the inlet and outlet ports with pillars near the inlet and outlet ports to retain the adsorbent (~2.3 mg Carbopack X). The  $\mu$ F chip has chromium/gold (Cr/Au) contact pads on its backside for resistive heating and a titanium/platinum (Ti/Pt) resistive temperature device to monitor temperature. The front-end sampling subsystem can attain preconcentration factors of five orders of magnitude.

Rapid heating of the  $\mu$ F to 225 degrees Celsius ( $^{\circ}$ C) desorbs retained compounds and “injects” them onto the two, 3m  $\mu$ columns (Figures 5d and 7; Reidy et al., 2006) for compound separation. The backsides of the  $\mu$ columns have Cr/Au heaters and Ti/Pt resistive temperature monitoring devices. Both columns can be independently temperature programmed. As compounds exit the  $\mu$ column they enter the micro-scale CR array detector (Figure 8) for detection by four different CR detectors. TCE calibration curves are shown in Figure 9. TCE LODs were in the sub-ppb range for 20 L samples. Chromatograms for an air sample containing TCE and 45 other compounds are also shown in Figure 9.



**Figure 7. Scanning electron microscope (SEM) images of the etched-silicon channels used in the 3-m-long  $\mu$ columns prior to sealing and coating with stationary phase.**

a) previous design, and b) current design (chamfered)

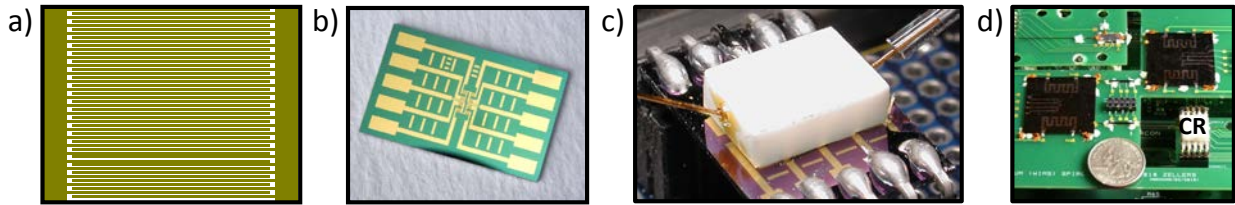


**Figure 8. Photographs of the CR array**

- a) interdigital electrodes (coated with MPN CRs),
- b) uncoated CR array chip, c) CR array with flow cell, and
- d)  $\mu$ GC-installed CR array

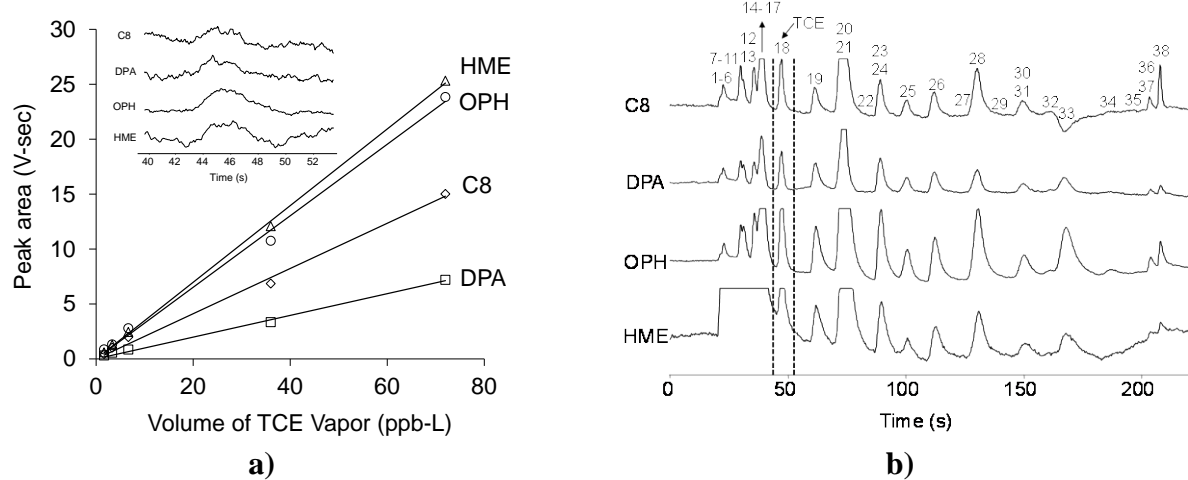


**Figure 9. a) TCE Calibration curves for  $\mu$ GC prototype (inset shows TCE peaks for 20 L 0.12 ppb TCE); and b) chromatograms from the four CR sensors for analysis of TCE and other VOCs.**

Co-elution of peaks can cause  $\mu$ GC prototype TCE results to be biased high. Lack of relative response patterns fidelity to the TCE pattern can be used to indicate the presence of co-eluting peaks. After the field demonstration, additional  $\mu$ GC laboratory testing was conducted using MCR to discern two closely eluting peaks, TCE and n-heptane (Kim and Zellers, in prep.); a component of gasoline, n-heptane is a common interferent.

### 6.3 FIELD TESTING

Field testing was primarily conducted from July 2010 to September 2010, and results are reported in Kim et al. (2012a & b). Figure 10 shows photographs of the study house. Preliminary field testing, including use of the HAPSITE portable GC/MS (courtesy of Kyle Gorder and Eric Dettenmair of Hill AFB), established that a crack in the basement in a small closet under the stairs was a significant TCE VI entry location. This proved useful to the  $\mu$ GC field demonstration since a wide range of indoor TCE concentrations could be established by inducing negative pressure in the house. The indoor temperature was  $25 \pm 3^\circ\text{C}$  and relative humidity was within the range of 20 to 60%.

Described in this report are all of the  $\mu$ GC and reference method (TO-15) TCE paired test results. Also included are selected temporal and spatial TCE monitoring results (along with concurrent TO-15 and HAPSITE results) to illustrate  $\mu$ GC prototype performance under fixed-location and portable operation mode applications. System blanks and field blanks were analyzed by the prototypes without sample collection and after collecting 2 L of VOC-free air from a cylinder, respectively. System blanks were comparable to VOC-air blanks.

Offline analysis of SPIRON chromatographic data was done by importing test files of retention times and sensor responses into GRAMS/32 AI (Ver. 6.0, Thermo Scientific, Waltham, Massachusetts). TCE peak heights and areas were extracted from the raw chromatograms using a Fourier self-deconvolution routine in GRAMS (Kauppinen et al., 1981). Subsequent data analysis was performed using Excel or Matlab (Ver. R2010a, MathWorks, Inc., Natick, Massachusetts).

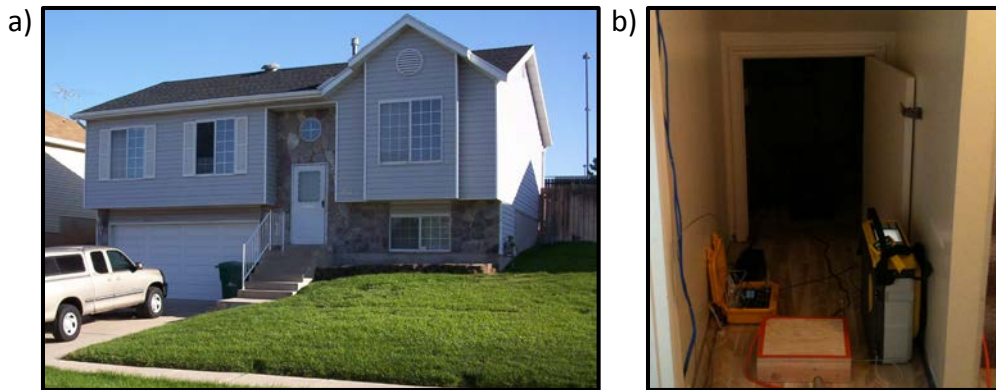


**Figure 10. Photographs of a) Layton, Utah, ASU SERDP project study house and b) basement storage closet beneath stairs with significant VI entry location.**

#### 6.4 FIELD SAMPLING METHODS

For fixed-location sampling, the  $\mu$ GC prototypes were located near the designated sampling locations with the  $\mu$ GC sample inlet connected via stainless steel tubing (internal volume less than 0.5% of sample volume) to the sampling location. Generally, the  $\mu$ GC prototypes sampling locations were: several inches from the storage closet floor crack and in the hallway outside of the storage closet several inches from the HAPSITE sampling location. For the portable mode sampling, the  $\mu$ GC was simply placed in the sampling location. TO-15 samples were taken with 6 L Summa canisters. Flow restriction was used to approximate the same sampling time window for the TO-15 samples as for the concurrent  $\mu$ GC samples. The canister inlet was placed within several inches of the concurrent  $\mu$ GC sampling location.  $\mu$ GC sample turnaround times were 30 minutes or less (depending upon preconcentration required). Differential pressure measurements were made using an Omnidigital<sup>TM</sup> 4 differential pressure transducer and recorder. One side of the pressure transducer was connected to tubing (sealed in the floor) exposed to sub-slab vapor, and the other side was exposed to indoor air.

## 6.5 FIELD SAMPLING RESULTS

Field-determined TCE calibration curves and relative response patterns for both  $\mu$ GC prototypes are shown in Figure 11 (generated using 0.5 to 8 L 9.6 ppb TCE). All curves were linear with a correlation coefficient ( $r^2$ ) of 0.98 or greater. Corresponding TCE LODs are given in Table 3. Although LODs vary by sensor, all sensors had sub-ppb LODs for 20 L samples. Responses for the TCE standardization gas varied modestly over the main 3-week field demonstration period as shown in Figure 12. TCE response factors were adjusted through the demonstration to account for the response variation. Chromatograms for a field sample are shown in Figure 13, TCE was confirmed as 12 ppb and several distinct peaks for other unknown compounds are also observed. The relative response patterns for some of these unknowns were markedly different from TCE's pattern while others were quite similar, illustrating the importance of retention time and development of a chlorinated compound-sensitive sensor for the array in TCE quantification.

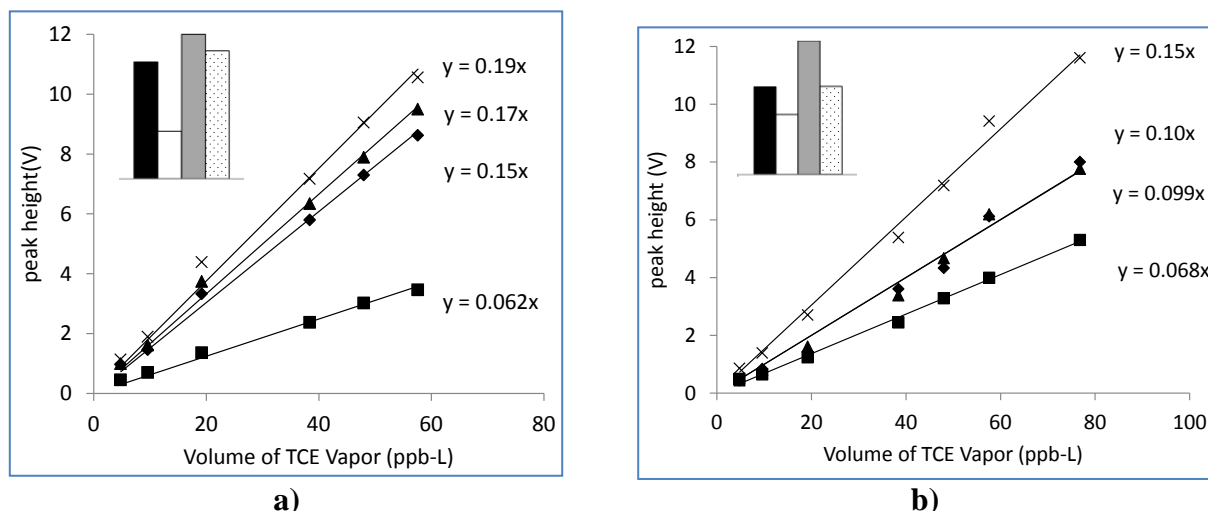


**Figure 11. Field TCE calibration curves.**

a) Prototype 1 and b) Prototype 2. Symbols:  $\times$  - OPH;  $\blacktriangle$  - HME;  $\blacklozenge$  - C8;  $\blacksquare$  - DPA. All regression lines have  $r^2$  values  $>0.98$ . Insets show the normalized response pattern for TCE from the CR arrays (bars left to right are: C8, DPA, OPH, and HME).

**Table 3. LOD for TCE with both  $\mu$ GC prototypes in the field for assumed sample volumes of 4 L and 20 L (in parentheses).**

Sensor	LOD (ppb)	
	Prototype 1	Prototype 2
C8	0.37 (0.073)	0.65 (0.13)
DPA	0.95 (0.19)	0.50 (0.099)
OPH	0.11 (0.022)	0.15 (0.029)
HME	0.11 (0.021)	0.30 (0.060)

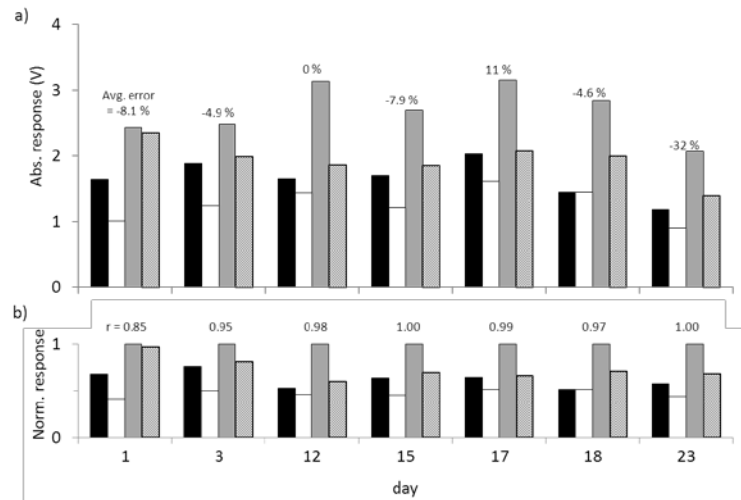


**Figure 12. Results of periodic analysis of the TCE tank standard (2 L sample; 9.6 ppb TCE) showing a) stability of responses and b) relative response patterns over the 3-week field study.**

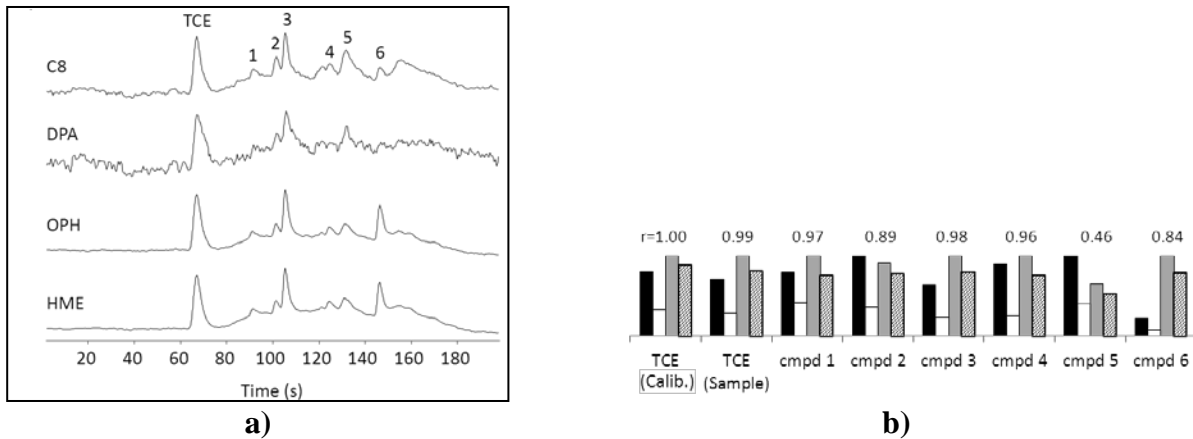


**Figure 13. a) Representative chromatograms from the MPN-coated CR array for a field measurement having 12 ppb TCE; and b) response patterns for TCE and unknown VOCs with pattern-matching correlation coefficients (r). Bars left to right: C8, DPA, OPH, and HME.**

TCE results for the  $\mu$ GC and concurrent TO-15 (reference method) data pairs are given in Figure 14. TCE concentrations ranged from sub-ppb to above 15 ppb. The correlation between the two methods was good in the higher concentration range, but showed a positive bias for the  $\mu$ GC results in the lower concentration range. A more detailed analysis of subsets of the TCE data pairs is shown in Figure 15 where: 1) TO-15 TCE concentration was greater than the MAL (2.3 ppb TCE at the time of the field demonstration) with response pattern correlation coefficients ( $r$ ) with the TCE standard greater than 0.85; 2) TO-15 TCE concentrations less than the MAL and  $r$  greater than 0.85; and 3) TO-15 TCE concentration less than the MAL and  $r$  less than 0.85. Results of the analyses show that the  $\mu$ GC was accurate for TCE above the MAL and reasonable pattern match ( $r > 0.85$ ) with TCE, less accurate below the MAL with a reasonable

pattern match with TCE, and the least accurate below the MAL and a poor pattern match ( $r < 0.85$ ) with TCE.

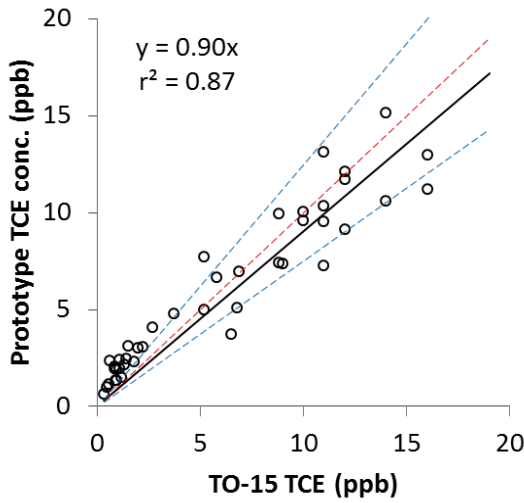


**Figure 14. Correlation of pooled TCE measurements from  $\mu$ GC prototypes and corresponding TO-15 samples. Black solid line is the forced-zero intercept linear regression (slope and  $r^2$  shown), red dotted line is 1:1 correlation, and blue dashed lines are  $\pm 25\%$  of 1:1.**

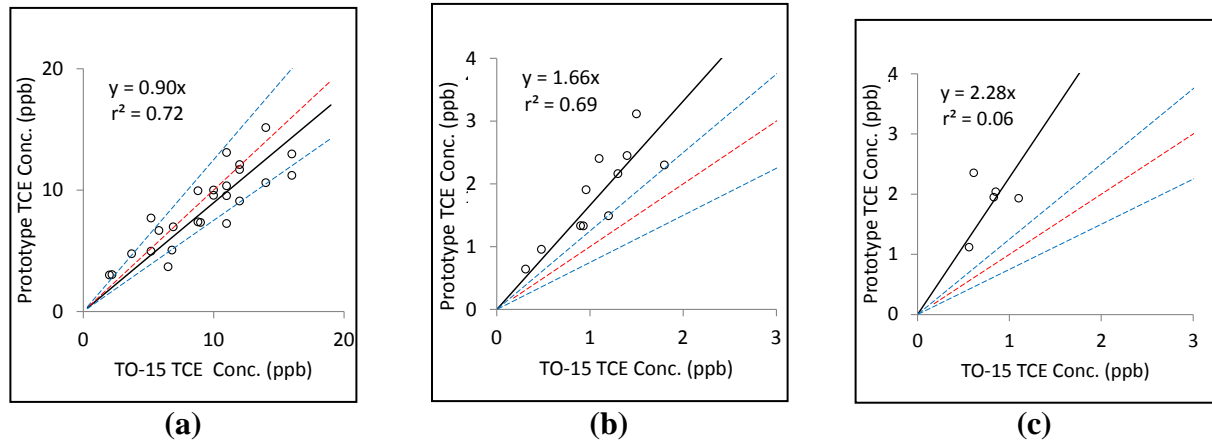


**Figure 15. Correlations of the pooled TCE measurements from  $\mu$ GC prototypes with corresponding TO-15 results for data pair subsets a) TCE > MAL and  $r > 0.85$ , b) TCE < MAL and  $r > 0.85$ , and c) TCE < MAL and  $r < 0.85$  (MAL 2.3 ppb at time of field demonstration). Lines as in Figure 14**

Results of the paired  $\mu$ GC and TO-15 data are consistent with co-elution of interferents with TCE in the lower concentration range. Figure 16 shows chromatogram subsections for a) TCE with good agreement with TO-15 and good TCE pattern match; b) distorted TCE peak with a poor TCE pattern match (co-elution); and c) distorted TCE peak with a good TCE pattern match (co-elution). Some interferent compounds have patterns similar to that of TCE. A corresponding chromatogram subsection for a VOC-free air blank is also shown.

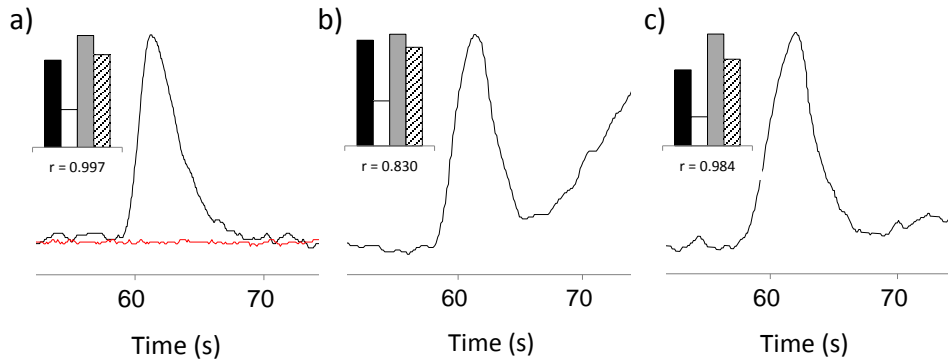


**Figure 16. Extracted subsections of several chromatograms from the OPH sensor of Prototype 1 and corresponding normalized response patterns from the CR array (insets) for TCE peaks**

a) without (-5% error; relative to TO-15) and b) & c) with co-eluting interferences (note peak distortions; +52 and +64% error, respectively), illustrating the utility of the pattern-matching criterion ( $r$  = pattern matching correlation coefficient). The red line is a VOC-free air blank.

An example of temporal data generated using the  $\mu$ GC prototypes is shown Figure 17; a 48-hour automated (unattended) run of both prototypes, one in the basement crawlspace with a significant VI entry location and the other in the nearby hallway. In addition, TO-15 results for the crawlspace and portable HAPSITE GC/MS results for the hallway are shown. Negative pressure was induced during two time periods which raised the TCE due to VI. There was generally good agreement between the three methods. During periods of positive indoor pressure elevated TCE levels were due a TCE source in the attached garage. The results indicate that when combined with wireless communications, the  $\mu$ GC would have utility as a long-term monitoring approach.

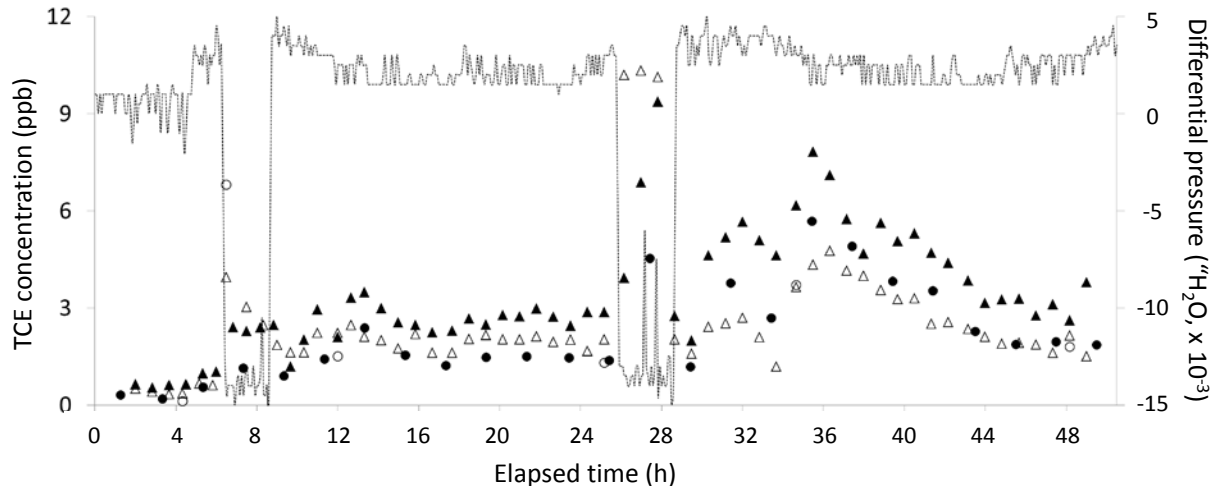


**Figure 17. Results of 48 hours of continuous, automated (unattended) TCE concentration measurements with Prototype 1 (open triangles, crawl space) and Prototype 2 (filled triangles, hallway), along with measurements by TO-15 (open circles, crawl space) and portable GC/MS (filled circles, hallway) as a function of differential pressure (indoor relative to sub-slab; line).**

An example of spatial monitoring using the  $\mu$ GC is shown in Figure 18 where an emplaced TCE source is located (in basement closet) in a house without TCE VI. Additionally, TCE gun solvent previously stored in the gun cabinet was also detected.

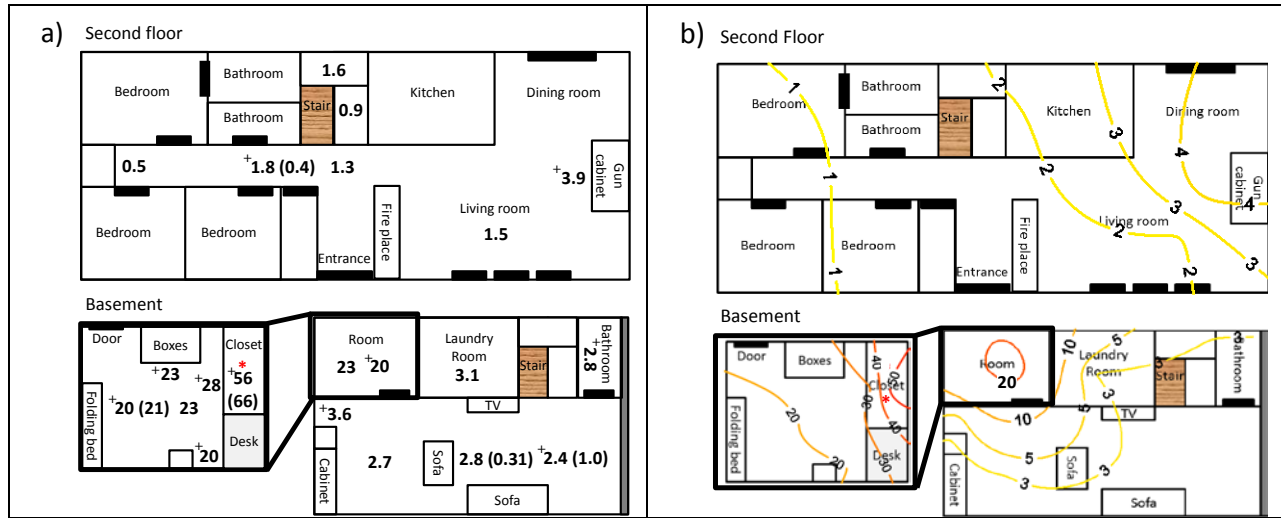


**Figure 18. Spatial distributions of TCE in Layton, Utah, house without VI and emplaced indoor source of TCE.**

a) sampling locations and TCE concentrations (ppb) determined by Prototype 1 and TO-15 (in parentheses) (Note: samples collected on Day 2 are denoted with a “+”) and b) contour map of Prototype 1 TCE concentrations (ppb). Lower left image shows an enlarged view of the room in the basement and the closet in which the TCE source was hidden (indicated by “\*”).

## 7.0 PERFORMANCE ASSESSMENT

The performance objective for the portable  $\mu$ GC mode sensitivity was the TCE LOD being less than or equal to 0.06 ppb TCE. LODs for Prototype 1 and Prototype 2 sensors are given in Table 3. A 10-L sampling period will be used since shorter turnaround times are more appropriate for a more rapid portable sampling situation. The 10-L TCE LOD for most sensitive sensor Prototype 1 and Prototype 2 are 0.04 ppb (HME) and 0.06 ppb (OPH), respectively. On the basis of the most sensitive sensor, the portable mode sensitivity performance objective would be met for both  $\mu$ GC prototypes. For pattern recognition, it is possible to use three sensors, so the highest LOD of the most sensitive three sensors for Prototype 1 and Prototype 2 give LODs of 0.15 ppb (C8) and 0.2 ppb (DPA), respectively. On the basis of sufficient sensors for pattern recognition, both  $\mu$ GC prototypes would not meet the portable mode sensitivity performance objective.

The performance objective for the fixed-location  $\mu$ GC mode sensitivity is the TCE LOD being less than or equal to 0.03 ppb TCE. A 20-L sampling period will be used due to more relaxed time constraints in the fixed location mode. The 20-L TCE LOD for Prototype 1 and Prototype 2 most sensitive sensor is 0.02 ppb (HME) and 0.03 ppb (OPH), respectively. On the basis of the most sensitive sensor, the fixed-location mode sensitivity performance objective would be met for both  $\mu$ GC prototypes. For pattern recognition, it is possible to use three sensors, so the highest LOD of the most sensitive three sensors for Prototype 1 and Prototype 2 give LODs of 0.07 ppb (C8) and 0.1 ppb (DPA), respectively. On the basis of sufficient sensors for pattern recognition, both prototypes would not meet the fixed-location mode sensitivity performance objective.

Performance evaluation of the  $\mu$ GC response stability is based upon the  $\mu$ GC responses to 2 L of the 9.6 ppb TCE gas standard (calibrations and standardization checks) over the primary 3-week field sampling period, with the goal of a relative standard deviation (RSD) of 20% or less. The RSD for Proto 1 and Proto 2 TCE responses were 21% and 17%, respectively. Although there was some variability in  $\mu$ GC response to TCE, it was relatively modest with the average RSD between the two prototypes being 19%; thus, the  $\mu$ GC response stability performance objective was met. As a practical note, the CR sensor array temperature is a significant factor in response stability, so increased temperature control of the detector will likely improve response stability (lab experience has shown that CR response varies with temperature).

Assessment of the degree of agreement between the  $\mu$ GC and TO-15 field sample TCE results is separated into two categories: 1) those where the TO-15 value is greater than 10 times the  $\mu$ GC LOD and those where the TO-15 value is less than 10 times the  $\mu$ GC LOD. For the greater than 10 times LOD category, performance success is to be within a factor of 1.43 (70 to 143%), with a 20% failure rate as acceptable. For the less than 10 times LOD category, performance success is to be within a factor of 2 (50 to 200%), with a 20% failure rate as acceptable. Performance results for both categories are given in Figure 19.

For the higher concentration range category (Figure 19a), there were 26 sample pairs with five pairs with the  $\mu$ GC TCE concentration exceeding the corresponding TO-15 TCE concentration by greater than a factor of 1.43 (70 to 143%), a 19% failure rate (lower than 20% acceptable

rate). The five samples that did exceed the 1.43 criterion were generally close to the criterion. For this higher concentration category, the  $\mu$ GC meets the performance evaluation criterion.

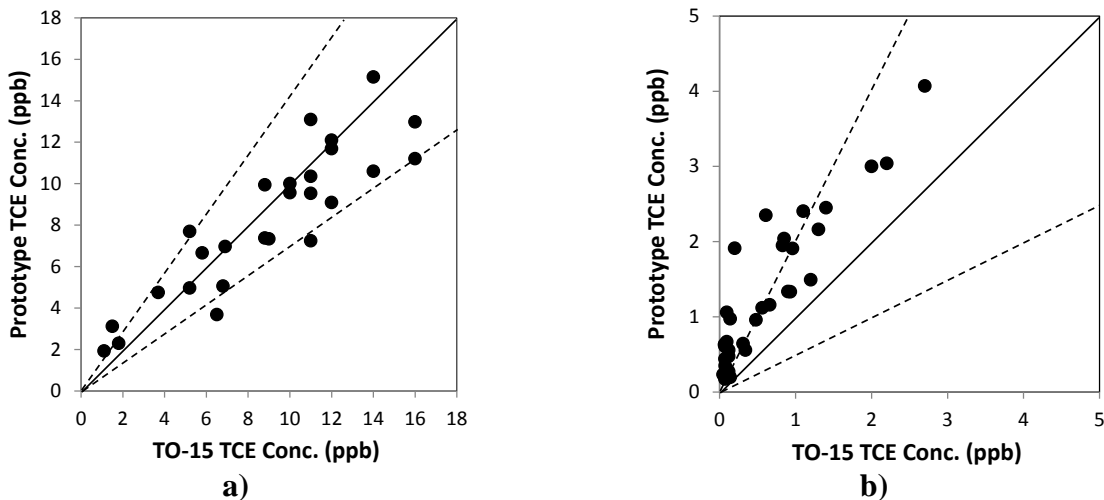


**Figure 19. Correlation between TO-15 and  $\mu$ GC prototype TCE field sample results for a) TO-15 results greater than 10 times  $\mu$ GC LOD, and b) TO-15 results less than 10 times  $\mu$ GC LOD.**

Dashed lines are  $\pm$  factor of 1.43 (143 – 70%) for a) and  $\pm$  factor 2.0 (200 – 50%) for b).

Performance results of the lower concentration category (Figure 19b) show a positive bias in the lower concentration range due to co-eluting peaks as discussed previously. Of the 33 sample pairs in this category, 19 samples were greater than the factor of 2 criterion, a failure rate of 58% (higher than 20% acceptable rate). For this lower concentration category, the  $\mu$ GC does not meet the performance evaluation criteria.

**Ease of Use:** Field team experience showed that a single field technician could effectively use the  $\mu$ GC in a field setting. It is anticipated that improvements made during  $\mu$ GC commercialization would significantly improve its ease of use. Rapid reduction of raw  $\mu$ GC data will be improved during commercialization allowing rapid quantification of sample analyses. Field standardization and blanks were easily accomplished. Development of an automated standardization method will improve the  $\mu$ GC's utility in long-term monitoring applications. Blanks using VOC-free air, scrubbed ambient air, or system blanks were easily accomplished.

**Rapid Site Assessment:** Field experience demonstrated that rapid site assessment was possible for the portable  $\mu$ GC mode. The emplaced TCE source was located in 1 day, although a second day was utilized to improve data resolution and replicate sampling. Commercialization will substantially improve the ability of the  $\mu$ GC for rapid site assessment.

**Long-term Operation:** The bulk of the  $\mu$ GC results reported were obtained over a 3-week period and  $\mu$ GC operation in the field was greater than 1 month. Long-term operation of the  $\mu$ GC was successfully demonstrated. Continuous 48-hour automated operation of the  $\mu$ GC demonstrated the capacity to operate in an automated fashion without continuous operator attention. Wireless

remote controlled operation of the  $\mu$ GC, as well as data retrieval, is anticipated to be fairly easily accomplished. A challenge will be development of an automated standardization check method.

## 8.0 COST ASSESSMENT

### 8.1 COST MODEL

The SPIRON  $\mu$ GC is a laboratory prototype and is not commercially available. Additional development is needed to bring a  $\mu$ GC like the SPIRON prototype to commercial production before being available for environmental applications such as VI. Thus, the cost of a potential commercial  $\mu$ GC for VI applications is currently unknown and estimated. The potential market size of  $\mu$ GCs for environmental and similar applications (e.g., industrial hygiene, public health) is also unknown, but potentially significant. Additional development work will be needed, including improvements to the CR sensor array, embedded microprocessor for data storage and preliminary data reduction (allowing independent operation from a laptop), wireless communications, robust field design, etc. Many of the commercial  $\mu$ GC parts will be relatively inexpensive to produce, especially the micro-fabricated components.

Considering the uncertainties in the potential cost of the  $\mu$ GC (with front-end module), it may be reasonable to assume that the upper end potential cost might be similar to the cost of a lower cost tabletop GC (e.g., SRI TO-14 Air Monitoring GC System, ~\$23,000, [www.srigc.com](http://www.srigc.com)). Potential  $\mu$ GC cost range might be \$5,000 to \$25,000, so a conservative estimate of \$20,000 will be assumed. Periodic  $\mu$ GC refurbishing will be required, as for all GCs. A military facility could purchase the  $\mu$ GCs. Direct purchase may be the most cost-effective approach depending upon the nature and magnitude of their VI-related issues. However, it may be more appropriate and useful to assume daily or monthly usage fees from an outside contractor. For the forensic VI  $\mu$ GC application assuming a 6-month usage cost recovery and \$1,000 refurbishing cost/30 field days gives an estimated usage rate of \$150/day. For the long-term VI  $\mu$ GC application assuming an 8-month usage cost recovery and \$500/month refurbishing cost gives an estimated usage rate of \$3,000/month. Simple cost models for use of a commercially produced  $\mu$ GC for short-term forensic or long-term monitoring VI applications are given below in Tables 4 and 5.

**Table 4. Cost model for short-term forensic-type application of  $\mu$ GC for VI.**  
(2 on-site days; second day to allow for removal of potential indoor sources and re-assessment)

Cost Element	Data / Information Assessed	Estimated Costs	
Short-term forensic application using $\mu$ GC	• Personnel required and associated labor (includes mobilization/demobilization; calibration & QA <sup>a</sup> / QC <sup>b</sup> )	Lab field technician, 30 hours	\$2,100
	• $\mu$ GC operation costs	Project engineer, 3 hours	\$300
	• Vehicle usage	$\mu$ GC, 2 days	\$300
		Vehicle, 2 days	\$120
Reporting	• Assume minimal reporting requirements	Lab field tech., 8 hours	\$560
		Project engineer, 2 hours	\$200
<b>Cost Estimate</b>			<b>\$3,580</b>

<sup>a</sup>quality assurance

<sup>b</sup>quality control

**Table 5. Cost model for long-term monitoring application of μGC for VI.**  
 (assumes 3 month operation; 12 samples per day; 2 system blanks daily;  
 4 standardization checks)

Cost Element	Data / Information Assessed	Estimated Costs	
Long-term monitoring of house using μGC	• Personnel required and associated labor (mobilization/demobilization; calibration and QA/QC)	Lab field technician, 120 hours	\$8,400
	• μGC costs (3 months)	Project engineer, 12 hours	\$1,200
	• Remote communications for system and results monitoring	μGC, 3 months	\$9,000
		Vehicle, 4 days	\$240
Reporting	• Assume minimal reporting requirements	Lab field tech., 16 hours	\$1,120
		Project engineer, 4 hours	\$400
<b>Cost Estimate</b>			<b>\$20,360</b>

## 8.2 COST DRIVERS

A key cost driver in selecting μGC technology (commercial production units) is the ability to accurately determine TCE concentrations in indoor air samples at relevant low concentrations with common indoor air interferents present. Although a challenging task, this demonstration has shown that sufficient accuracy can be achieved for TCE indoor air VI in the several ppb range and higher; with further modifications/optimization the level at which TCE can be accurately determined in indoor air should be lowered by an order of magnitude.

## 8.3 COST ANALYSIS

The current approach for indoor air VI investigations is to collect canister samples, followed by shipment to an environmental air analysis laboratory for TO-15 GC/MS analysis. A difficulty in making a direct comparison between using the μGC and using traditional TO-15 is that data density cannot be matched by traditional TO-15 (except at extraordinary cost). Considering that the two methods are so different, it is reasonable to expect that, even if μGC technology were used, a minor amount of TO-15 confirmatory sampling might be appropriate.

Although not directly comparable, the short-term forensic TO-15 approach cost estimate is \$7,820 compared with \$3,580 for the μGC approach. The TO-15 approach is largely impractical for forensic determination of indoor sources. The cost comparison for the long-term monitoring type application uses an automated canister sampler capable of filling seven canisters with one canister taken per day, minimizing the intrusive nature of the investigation. The cost estimate for the long-term TO-15 approach is \$45,140, compared to the \$20,360 cost estimate for the long-term monitoring μGC approach. The TO-15 approach provides only one sample per day, whereas the μGC provides 12 or more samples per day. The μGC provides a significant cost and information advantage over the TO-15 approach. If a lower sampling density for TO-15 was adequate to meet sampling objectives, the TO-15 approach may be cost competitive.

## 9.0 IMPLEMENTATION ISSUES

A  $\mu$ GC prototype was used in this demonstration project to detect TCE in indoor air for VI applications. The  $\mu$ GC prototype was able to detect TCE due to VI in indoor air, with more accurate values obtained at the higher TCE levels and less accurate (positive bias) at the lower levels. Continued development is needed to improve the accuracy at the lower levels for routine application of  $\mu$ GC technology to VI applications. Although challenging, attaining dependable analytical accuracy in the lower levels should be achievable (increased chromatographic resolution, detector and data reduction modifications).

The foremost, and overriding, implementation issue is that a fully developed, commercially available  $\mu$ GC that can be used in low concentration environmental applications such as VI is not currently available. Some  $\mu$ GCs (or partial  $\mu$ GCs) are available for petrochemical and natural gas industrial applications where quite high concentrations are the norm. A potential implementation issue since the field demonstration is that the Hill AFB TCE MAL lowered from 2.3 to 0.38 ppb, which will require instrumentation with sufficient accuracy at lower levels. The current project shows that it should be possible to produce a commercially available  $\mu$ GC for low concentration environmental applications and will hopefully encourage developments towards that goal.

USEPA is currently in the process of revising its 2002 Draft Subsurface Vapor Intrusion Guidance with a final version to be released by November 2012 (USEPA, 2010). In revision of the guidance, USEPA (2010) indicated that an increased emphasis on indoor air sampling for spatial and temporal monitoring will be included in the final version of the VI guidance.

The prototype  $\mu$ GC was not capable of rapid data collection in the field as currently configured. Microprocessor development is needed to store and process data as it is being gathered. Additionally, the development of easy-to-use software for interfacing with the  $\mu$ GC via remote communications, including robust data reduction, would facilitate implementation of  $\mu$ GC technology by reducing manpower requirements.

The stability of the CR array also remains an issue. The results from this demonstration showed that, after some initial changes in sensor sensitivity, they tended to become stable (unknown for how long). These CR array results were encouraging. The CR array would benefit from the development of a sensor that was particularly sensitive to chlorinated compounds (such as TCE) to aid in the use of MCR to differentiate TCE from non-chlorinated compounds, which are likely causing interference; development of a chlorinated compound-specific CR sensor is unknown at this time. Relative response patterns for TCE and some of the common non-chlorinated compounds that elute near TCE are similar to each other, so greater differentiation would be beneficial. The CR arrays are coated by hand, each individually; mass production will lead to more uniformity in CR array performance.

USEPA's Environmental Technology Verification (ETV) Program is designed to accelerate the entrance of new environmental technologies into domestic and international marketplaces, and has successfully been used for environmental sensors and field analytical technologies. The ETV program would be appropriate for a commercial  $\mu$ GC with environmental applications.

*This page left blank intentionally.*

## 10.0 REFERENCES

Agency for Toxic Substances and Disease Registry (ATSDR), 1997. Toxicological Profile for Trichloroethylene, Agency for Toxic Substances and Disease Registry, [www.atsdr.cdc.gov/toxprofiles/tp19.html](http://www.atsdr.cdc.gov/toxprofiles/tp19.html).

Colorado Department of Public Health and Environment (CDPHE), 2005. Trichloroethylene Health Effects Fact Sheet, Colorado Department of Public Health and Environment, [www.cdphe.state.co.us/HM/tcef.pdf](http://www.cdphe.state.co.us/HM/tcef.pdf).

Gorder, K.A., and E.M. Dettenmaier, 2011. Portable GC/MS Methods to Evaluate Sources of cVOC Contamination in Indoor Air, *Ground Water Monitoring and Remediation*, 31:113-119.

Kauppinen, J.K., D.J. Moffatt, H.H. Mantsch, and D.G. Cameron, 1981. Fourier Self-Deconvolution: A Method for Resolving Intrinsically Overlapped Bands, *Appl. Spectrosc.*, 35:271-276.

Kim, S.K., H. Chang, and E.T. Zellers, 2011. Microfabricated Gas Chromatograph for the Selective Determination of Trichloroethylene Vapor at Sub-Parts-Per-Billion Concentrations in Complex Mixtures, *Analytical Chemistry*, 83(18):7198-7206.

Kim, S.K., H. Chang, J. Bryant, D.R. Burris, and E.T. Zellers, 2012(a). Microfabricated Gas Chromatograph for On-Site Determinations TCE Arising from Vapor Intrusion Studies, Part I: Field Evaluation, *Environ. Sci. Technol.*, 46(11):6065-72.

Kim, S.K., D.R. Burris, H. Chang, J. Bryant-Genevier, K.A. Gorder, E.M. Dettenmaier, and E.T. Zellers, 2012(b). Microfabricated Gas Chromatograph for On-Site Determinations TCE Arising from Vapor Intrusion Studies, Part II: Temporal/Spatial Monitoring, *Environ. Sci. Technol.*, 46(11):6073-6080.

Kim, S.K., and E.T. Zellers, *In Preparation*. Multivariate Curve Resolution of Partially Resolved Analytes Measured with a Micro-Scale GC and Microsensor Array Detector.

Reidy, S., G. Lambertus, J. Reece, and R. Sacks, 2006. High-Performance, Static-Coated Silicon Microfabricated Columns for Gas Chromatography, *Anal. Chem.*, 78, 2623-2630.

Sukaew, T., H. Chang, G. Serrano, and E.T. Zellers, 2011. Multi-Stage Preconcentrator/Focuser Module Designed to Enable Trace Level Determinations of Trichloroethylene in Indoor Air with a Microfabricated Gas Chromatograph, *Analyst*, 136:1664-1674.

U.S. Environmental Protection Agency (USEPA), 2002. OSWER Draft Guidance for Evaluating the Vapor Intrusion to Indoor Air Pathway from Groundwater and Soils (Subsurface Vapor Intrusion Guidance), EPA-D-02-004.

USEPA, 2010. OSWER Review Document regarding the 2002 Draft Subsurface Vapor Intrusion Guidance, [www.epa.gov/oswer/vaporintrusion/documents/review\\_of\\_2002\\_draft\\_vi\\_guidance\\_final.pdf](http://www.epa.gov/oswer/vaporintrusion/documents/review_of_2002_draft_vi_guidance_final.pdf).

## APPENDIX A

### POINTS OF CONTACT

<b>Point of Contact</b>	<b>Organization</b>	<b>Phone Fax E-Mail</b>	<b>Role In Project</b>
H. James Reisinger	IST 4940 Cowan Rd. Acworth, GA 30101	Phone: 770-425-3080 ext. 102 Fax: 770-425-0295 E-mail: istatlanta@aol.com	Principal Investigator (PI)
David R. Burris, Ph.D.	IST 228 Harrison Ave., #102 Panama City, FL 32401	Phone: 850-522-8005 Fax: 850-522-8060 E-mail: dave@burris-net.com	Co-PI; University of Michigan Liaison; Demonstration Coordinator
Edward T. Zellers, Ph.D.	University of Michigan Department of Environmental Health Sciences School of Public Health Room M6543 109 S. Observatory St. Ann Arbor, MI 48109	Phone: 734-936-0766 Fax: 734-763-8095 E-mail: ezellers@umich.edu	Development, Fabrication, and Testing of $\mu$ GC
Kyle Gorder	75 CEG/CEVR, Environmental Restoration Branch 7274 Wardleigh Road Hill AFB, UT 84056	Phone: 801-775-2559 E-mail: kyle.gorder@hill.af.mil	Hill AFB POC; Demonstration Facilitator
Robert E. Hinchee, Ph.D., P.E.	IST 1509 Coastal Highway Panacea, FL 32346	Phone: 850-984-4460 Fax: 850-984-4467 E-mail: rob@hinchee.org	Advisor; Initial Project PI



**ESTCP Office**  
4800 Mark Center Drive  
Suite 17D08  
Alexandria, VA 22350-3605  
(571) 372-6565 (Phone)  
E-mail: [estcp@estcp.org](mailto:estcp@estcp.org)  
[www.serdp-estcp.org](http://www.serdp-estcp.org)